International Journal of Solids and Structures 51 (2014) 1164–1174

Contents lists available at ScienceDirect

International Journal of Solids and Structures

journal homepage: www.elsevier.com/locate/ijsolstr

Constitutive modeling of biodegradable polymers: Hydrolytic degradation and time-dependent behavior

André C. Vieira [a,*], Rui M. Guedes [b], Volnei Tita [a]

[a] Aeronautical Engineering Department, São Carlos School of Engineering, University of São Paulo, Av. João Dagnone n.1100, 13.573-000 São Carlos, São Paulo, Brazil
[b] Mechanical Engineering Department, Faculty of Engineering of University of Porto, Rua Dr Roberto Frias s/n, 4200-465 Porto, Portugal

ARTICLE INFO

Article history:
Received 17 September 2013
Received in revised form 5 November 2013
Available online 14 December 2013

Keywords:
Constitutive models
Time-dependent behavior
Biodegradable polymers
Functional compatibility

ABSTRACT

A large range of biodegradable polymers has been used to produce implantable medical devices. Apart from biological compatibility, these devices shall be also functional compatible and perform adequate mechanical temporary support during the healing process. However, the mechanical behavior of biodegradable materials during its degradation, which is an important aspect of the design of these biodegradable devices, is still an unexplored subject. Based on the literature, the mechanical behavior of biodegradable polymers is strain rate dependent and exhibits hysteresis upon cyclic loading. On the other hand, ductility, toughness and strength of the material decay during hydrolytic degradation. In this work, it is considered a three-dimensional time-dependent model adapted from the one developed by Bergström and Boyce to simulate the performance of biodegradable structures undergoing large deformations incorporating the hydrolysis degradation. Since this model assumes that the mechanical behavior is divided into a time independent network and a non-linear time-dependent network, it enables to simulate the monotonic tests of a biodegradable structure loaded under different strain rates. The hysteresis effects during unloading–reloading cycles at different strain levels can be predicted by the model. A parametric study of the material model parameters evolution during the hydrolytic degradation was conducted to identify which parameters are more sensible to this degradation process. The investigated model could predict very well the experimental results of a blend of polylactic acid and polycaprolactone (PLA–PCL) in the full range of strains until rupture during hydrolytic degradation. From these results and analyses, a method is proposed to simulate the three-dimensional mechanical behavior during hydrolytic degradation.

1. Introduction

Biodegradable polymers can be obtained from renewable resources or from chemical synthesis. A large range of mechanical properties and degradation rates are possible among these polymers. However, the prediction of the mechanical behavior of the biodegradable devices is fairly complex, because not only the mechanical properties evolve during degradation, but also these devices operate under large strain deformation fields. Due to the nonlinear response of the stress vs. strain relation, the classical linear elastic model is not valid for simulation under large strains. Current designs of biodegradable devices have been carried out by considering elastic or elastoplastic behavior and neglect any changing on the mechanical behavior caused by degradation (Moore et al., 2010). For many biomedical applications, the biodegradable polymeric structures are submitted to cyclic loading above the elastic limit. Hence, they are prone to accumulate plastic strain at each cycle, which may lead to laxity and consequent failure, such as in ligament augmentation devices (Vieira et al., 2009). For instance, Grabow et al. (2007) showed that significant creep of polylactides (PLA) under a constant load leads to strain accumulation and collapse.

Concomitantly to its nonlinear response, the mechanical behavior of polymeric materials is also temperature and rate dependent (Bardenhagen et al., 1997). However, in this work, only the rate dependent influence has been investigated. Temperature dependence may be neglected since isothermal hosting environment is always verified. The blend of polylactic acid and polycaprolactone (PLA–PCL), has been evaluated in previous works by the authors (Vieira et al., 2011a,b, 2013). The nonlinear viscoelastic characteristics of PLA were also verified by Soares (2008) and Grabow et al. (2007). The mechanical behavior of biodegradable polymers, such as PLA–PCL, also exhibits hysteresis, i.e. energy dissipation in form of heat, upon cyclic loading (Vieira et al., 2013). Therefore, time-dependent constitutive models are required to simulate such phenomena.

---

* Corresponding author. Tel.: +55 411633718612; fax: +55 1633738346.
E-mail addresses: avieira@inegi.up.pt (A.C. Vieira), rmguedes@fe.up.pt (R.M. Guedes), voltita@sc.usp.br (V. Tita).

0020-7683/$ - see front matter © 2013 Elsevier Ltd. All rights reserved.
http://dx.doi.org/10.1016/j.ijsolstr.2013.12.010

A constitutive model for a mechanical analysis is a relationship between the response of a body (for example, strain state) and the stress state due to the forces acting on the body, which can include the environmental effects. The actual models can be divided into two categories: the time-independent models and the time-dependent models (Ferry,1980). Several constitutive models have been proposed for non-degraded polymers and elastomers. Most of the earlier research works (Flory, 1977; James and Guth, 1943; Treloar, 1975; Wall and Flory, 1951) was devoted to the prediction of the time-independent response. Other more successful models are the 8-chain network model developed by Arruda and Boyce (1993a), and more recently the micro-sphere model developed by Miehe et al. (2004).

As observed in polymers, it is known that the stress in a biodegradable polymer will relax towards an equilibrium state after being subjected to a strain-step (Miller and William, 1984). This relaxed state has been simulated by linear elastic, elasto-plastic or hyperelastic models, but disregarding the rate dependency effect. Mechanical properties of biodegradable polymers are commonly assessed within the scope of linearized elasticity, despite the large strains, which are observed before material fracture. Classical models such as the neo-Hookean and Mooney–Rivlin models, usually applied for incompressible hyperelastic materials, have been used to predict mechanical behavior until rupture of non-degraded PLA (Garlotta, 2001; Lunt, 1998) under quasi-static monotonic loading. However, all of them neglect changes in the properties of the material during degradation process.

To consider time dependency, dissipative elements described by time inhomogeneous relations must be used in the model formulation. The simplest viscoelastic models consider a linear combination of springs (using the Hooke's law) and dashpots (using Newtonian damper with linear viscosity). The classical examples of these simple models are the Maxwell and Kelvin–Voigt models, in which spring and dashpots are organized in series or in parallel, respectively. More complex variants of these simple models can be found at the literature (Arruda and Boyce, 1993b; Bardenhagen et al., 1997; Bergström et al., 2002; Boyce et al., 1988; Dafalias, 1991; Drozdov and Gupta, 2003; Fancello et al., 2006; Harren, 1995; Hasan and Boyce, 1995; Hausler and Sayir, 1995; Holzapfel, 1996; Johnson et al., 1995; Lubarda et al., 2003; O'Dowd and Knauss, 1995; Reese and Govindjee, 1998; Rubin, 1987; Zdunek, 1993). These models can simulate the non linear viscoelastic, viscoplastic and hysteretic response of polymers. They are based on the concept of networks, combining elastic, sliding and dissipative elements, in order to simulate the time-dependent response of the material.

From the author's knowledge, only few methods were developed to predict the mechanical behavior during hydrolytic degradation. Those methods are based on hyperelastic models (Soares et al., 2010; Vieira et al., 2011a), or on quasi-linear viscoelastic models (Muliana and Rajagopal, 2012), or on phenomenological viscoplastic models (Khan and El-Sayed, 2012). However the calibration and validation of those methods were restricted to moderate deformations. Albeit, the Bergström–Boyce model (Bergström and Boyce, 1998) is a viscoelastic model, which simulates the performance of polymers undergoing large deformations. Since it is a physical inspired polymer model, it can be calibrated through a relative small set of simple mechanical tests, such as uniaxial loading, to provide accurate predictions for different loading cases (Bergström et al., 2002). These comprise monotonic loading under different strain rates, including hysteresis effect, and unloading–reloading cycles at different strain levels (Bergström et al., 2002).

Considering the latest arguments, a parametric study based on the adapted Bergström–Boyce model is performed in this work for a polymeric blend of PLA–PCL. Thus, the evolution of the material model parameters during hydrolytic degradation is determined, analyzing those parameters more sensible to this degradation process. Therefore, the limitation and potentialities of the adapted Bergström–Boyce model to simulate a biodegradable polymer over large range deformations under hydrolytic biodegradation are evaluated and discussed. Finally, a new method is proposed, based on these analyses, to simulate the three-dimensional time-dependent mechanical behavior during hydrolytic degradation. Although the present approach is applied to a PLA–PCL blend by using experimental data, the authors verified the applicability of the proposed method for other biodegradable polymers, such as polydioxone (PDO) and polyglycolic acid (PGA), which also exhibit time-dependent mechanical behavior. In a previous work (Vieira et al., 2010), it is possible to find experimental results for monotonic tensile tests during degradation. The application of the method proposed in this work will be addressed in the following papers.

2. Hydrolytic degradation

In general, the most important degradation mechanism for biodegradable polymers in biomedical applications is chemical degradation via hydrolysis or enzyme-catalyzed hydrolysis (Göpferich, 1996). It is well known that the mechanical behavior will evolve during time (see Fig. 1a), due to hydrolytic chain scission in the polymeric macromolecules. The reduction of molecular weight is linked to this evolution in mechanical response of biodegradable polymers (see Fig. 1b).

Hydrolysis has been traditionally modeled by using a first order kinetics equation based on the random scission kinetic mechanism of hydrolysis, according to the Michaelis–Menten scheme (Bellenger et al., 1995). Each polymer molecule, with its own carboxylic and alcohol end groups, is broken in two, randomly in the middle at a given ester group. So, the number of carboxylic end groups will increase with degradation time, while the molecules are being split by hydrolysis. The following first-order equation describes the hydrolytic process (Farrar and Gilson, 2002), in terms of the rate of formation of carboxyl end groups:

$$\frac{dc}{dt} = kewc = uc \tag{1}$$

where e, c and w are the concentrations of ester groups, carboxyl groups and water in the polymer, respectively. k is the hydrolysis rate constant and t is the degradation time. u is the hydrolytic degradation rate of the material, that can be determined by measuring strength or molecular weight evolution during hydrolytic degradation (see Vieira et al., 2011a). Since the concentration of carboxyl end groups is given by $c = 1/M_n$, where M_n is the number-average molecular weight of the polymer, the evolution of the , number-average molecular weight is given, after integration, by:

$$M_{n_t} = M_{n_0} e^{-ut} \tag{2}$$

It has been shown by Vieira et al. (2011a) that the fracture strength σ during degradation has a similar evolution to the number-average molecular weight of the polymer (see Fig. 1b), and can be predicted by the following equation:

$$\sigma_t = \sigma_0 e^{-ut} = \sigma_0 e^{-kwet} \tag{3}$$

where σ_t and M_{n_t} are the strength and the number-average molecular weight of the polymer at degradation time t; σ_0 and M_{n_o} are the corresponding initial (non-degraded) values. In Fig. 1a) is shown the mechanical response to uniaxial monotonic tensile tests until rupture, of PLA–PCL fibers during hydrolytic degradation. The evolution of fracture strength, according to Eq. (3), is similar to the evolution of the number-average molecular weight of the polymer (see Fig. 1b) in accordance to Eq. (2). In a semi logarithmic representation of

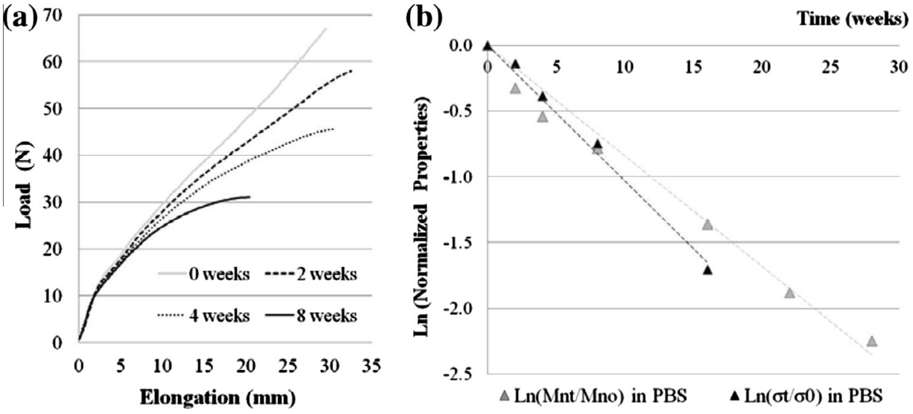

Fig. 1. (a) Monotonic tensile test results during hydrolytic degradation of PLA–PCL fibers; and (b) evolution of the normalized strength and molecular weight during degradation of PLA–PCL fibers (adapted from Vieira et al. (2011a)).

normalized strength or number-average molecular weight vs. degradation time, the degradation rate u corresponds to the slope of the linear fit. Further details of this degradation study can be found in Vieira et al. (2011a).

Degradation rate u is affected by the temperature or mechanical stress, molecular structure, ester group density as well as by the degradation media. Temperature will increase the hydrolysis rate constant k, which is associated to the probability of bond scissions, due to excitement of the molecules. In this work, the temperature is kept constant as in the human body, i.e. at the homeostatic value around 37 °C. However, it is important to highlight that the influence of the mechanical environment in the degradation rate has been also reported at literature (Chu, 1985; Miller and William, 1984). Similarly to temperature, stress applied during the degradation process also increases the probability of bond scissions and consequently increases the degradation reaction rate constant k. Some studies on rubbery polymers include the effect of microstructural changes in the polymer's macromolecules, crosslinks and entanglements, e.g. (Huntley et al., 1996; Rajagopal et al., 2007; Rajagopal and Wineman, 1992; Shaw et al., 2005; Smeulders and Govindjee, 1999; Wineman and Min, 2002). In these approaches, not specifically related to hydrolytic degradation, microstructural changes depend on state variables that locally measure chain stretches. Later, other researchers (Muliana and Rajagopal, 2012; Soares, 2008; Soares et al., 2010; Khan and El-Sayed, 2012) developed their methodologies based on these works, to introduce the influence of the strain field in the hydrolytic degradation. However, in the present work, no loads were applied during the degradation process. Concerning the degradation dependence of the investigated materials, some authors reported that the degradation rate of PLA and blends of PLA–PCL was significantly affected by some enzymes (Gan et al., 1999; Williams, 1981). The pH of the aqueous media also affects the degradation reaction rates constant k (Tsuji and Ikada, 1998, 2000; Tsuji and Nakahara, 2001). Again, in the present work, pH can be considered constant, because, pH is kept at a homeostatic value in the human body. In this work, it was assumed that the hydrolysis rate k was constant over time due to constant temperature, load (i.e. stress field equal to zero) and degradation media. Since water diffusion is much faster than hydrolysis, it is usually assumed that water is spread out uniformly in the sample volume (i.e. no diffusion control) (Li et al., 1990). Hence w was also assumed constant in the early stages of the reaction along the volume. In this early stage of erosion, when mechanical strength reduces significantly, the concentration of ester groups e located at the backbone chains is nearly constant. Despite of the scissions, which occur randomly in the ester groups, the macromolecules remain large (Göpferich and Langer, 1993). Therefore, the degradation rate, $u = kwe$, was considered constant during the whole process. In some cases, this assumption is not valid, because of heterogeneous diffusion, or due to the presence of a complex three-dimensional stress field, which evolves during the degradation process. However, it is possible to locally relate hydrolytic damage with strength and molecular weight. Thus, the hydrolytic damage d_h was defined by Vieira et al. (2011a), according to equation:

$$d_h = 1 - \frac{\sigma_t}{\sigma_0} = 1 - \frac{M_{n_t}}{M_{n_0}} = 1 - e^{-ut} \tag{4}$$

Hence, in order to simulate the evolution of the mechanical behavior of biodegradable polymers, the constitutive models must be adapted accordingly to hydrolytic damage d_h.

Recent developments of hyperelastic constitutive models enable the modeling of biodegradable structures during degradation (Soares et al., 2010; Vieira et al., 2011b) by assuming that the constitutive model parameters have been changed according to hydrolytic damage. More recently, a nonlinear viscoelastic model was used to simulate the time-dependent performance of biodegradable structures (Muliana and Rajagopal, 2012). As refereed previously, in that work, the authors considered that hydrolytic damage depends on the deviatoric strain tensor and the concentration of water. The degradation time-dependent phenomenon couples with the time-dependent mechanical behavior of the material. Stretching induces stress relaxation with time by means of viscous flow of the material. Simultaneously, stretching induces chemical scissions of the molecules, which provide an additive pathway for relaxation (Khan and El-Sayed, 2012). This approach simulates the relaxation behavior (or creep) during degradation reasonably well under moderate deformations. However, in many applications, the mechanical behavior of biodegradable polymers should be analyzed based on a finite strain theory (Khan and El-Sayed, 2012). On that ground, Khan and El-Sayed (2012) developed a phenomenological constitutive viscoelastic–plastic model, which was able to predict the response of biodegradable polymers under large deformations. The model consists on a nonlinear elastic spring element acting in parallel with a variable number of Maxwell elements. The hyperelastic response of both springs in the elastic branch and in the Maxwell branch is governed by the Ogden-type free energy function. The model was based on the phenomenological approach and some of its capabilities, mainly under large deformations, require experimental validation. These are the reasons because, in the present work, a method physically inspired on the hydrolysis random scission kinetics (particularly the hydrolytic degradation damage), and based on a phenomenological time-dependent model, was calibrated and validated under large deformations, considering hydrolytic degradation. It is important to mention that these approaches allow the four-dimensional modeling, where the degradation time is the fourth dimension.

3. Constitutive model

The non-linear and time-dependent mechanical behavior of a biodegradable polymeric blend of polylactic acid (PLA) and poly caprolactone (PCL) in proportion 90:10 was reported earlier Vieira et al. (2013). To address these observations, the Bergström and Boyce (1998) constitutive model was used and adapted in this work. In this constitutive model, the mechanical behavior is decomposed into two parts: a time-independent response, modeled by a hyperelastic constitutive model (defined as Network A), and a time-dependent deviation from equilibrium relaxed configuration, defined by a constitutive model (defined as Network B), which represents the inelastic strains, as shown by Fig. 2. In fact, the Network B is composed of an elastic element (also modeled by a hyperelastic constitutive model) in series with a time-dependent element, which acts to relieve the strain of the Network A in function of the time. According to the rheological representation of the constitutive model, shown in Fig. 2, the material behavior is modeled as two polymer networks acting in parallel (Bergström and Boyce, 1998) (see Fig. 3).

Since deformation in Network A is the same of Network B, then the deformation gradient $\mathbf{F} = \mathbf{F}_A = \mathbf{F}_B$. The deformation gradient in Network B can be further decomposed into a inelastic deformation followed by an elastic deformation ($\mathbf{F}_B = \mathbf{F}_B^e\mathbf{F}_B^i$), where the inelastic deformation represents the configuration obtained by a complete virtual elastic unloading of Network B under a stress free state.

The response of Network A is given by the Arruda–Boyce model (Arruda and Boyce, 1993a), also known as eight-chain model. The Cauchy stress tensor, $\mathbf{T}_A$, acting in Network A is given:

$$\mathbf{T}_A = \frac{\mu}{J\overline{\lambda^*}} \frac{\mathcal{L}^{-1}(\overline{\lambda^*}/\lambda_L)}{\mathcal{L}^{-1}(1/\lambda_L)} \mathrm{dev}[\mathbf{B}^*] + \kappa[\ln J]\mathbf{I} \tag{5}$$

where μ is the shear modulus, κ is the bulk modulus, and λ_L is the limiting chain stretch. I is the second order identity tensor. $\mathcal{L}^{-1}(x)$ is the inverse Langevin function, where $\mathcal{L}(x) = [\coth(x) - 1/x]$. The Jacobian is defined as $J = \det[F]$. $\overline{\lambda^*}$ is the applied chain stretch, which can be calculated from:

$$\overline{\lambda^*} = \sqrt{\frac{\mathrm{tr}(\mathbf{B}^*)}{3}} \tag{6}$$

where $B^* = J^{-2/3}B = J^{-2/3}FF^T$. The Cauchy stress tensor, $\mathbf{T}_B$ on Network B is also given by the eight-chain model:

$$\mathbf{T}_B = \frac{s\mu}{J_B^e\overline{\lambda_B^{e*}}} \frac{\mathcal{L}^{-1}\left(\overline{\lambda_B^{e*}}/\lambda_L\right)}{\mathcal{L}^{-1}(1/\lambda_L)} \mathrm{dev}\left[\mathbf{B}_B^{e^*}\right] + \kappa\left[\ln J_B^e\right]\mathbf{I} \tag{7}$$

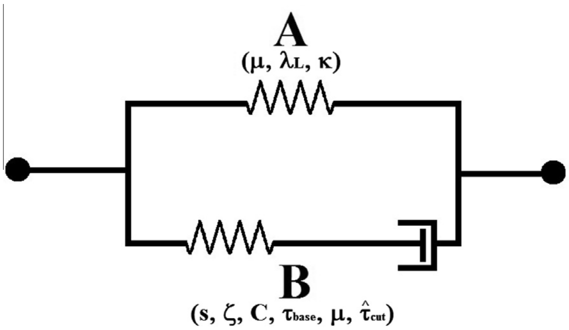

Fig. 2. Rheological representation adapted from Bergström and Boyce (1998).

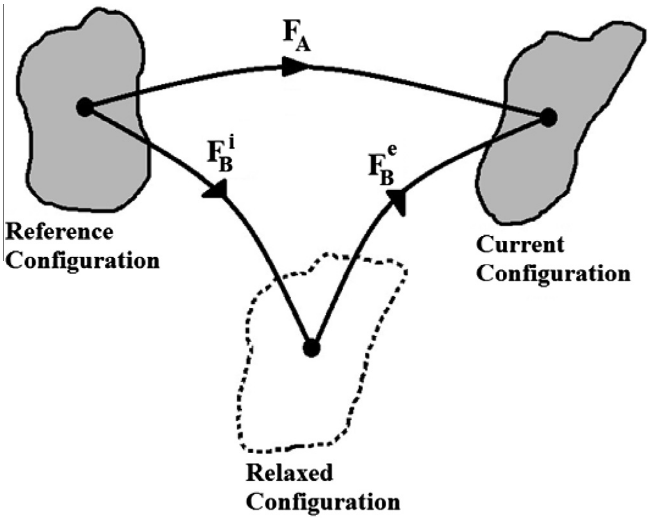

Fig. 3. Model deformation map adapted from Bergström and Boyce (1998).

where s is a dimensionless material parameter, which specifies the shear modulus of Network B relative to Network A, and $\overline{\lambda_B^{e*}}$ is the chain stretch in the elastic part of Network B. Using this representation, the total Cauchy stress tensor is given by $\boldsymbol{\sigma} = \boldsymbol{\sigma}_A + \boldsymbol{\sigma}_B$. The velocity gradient in Network B, $\mathbf{L}_B = \dot{\mathbf{F}}_B\mathbf{F}_B^{-1}$, and the deformation gradient in Network B can be decomposed into elastic and inelastic components ($\mathbf{F}_B = \mathbf{F}_B^e\mathbf{F}_B^i$). Hence:

$$\begin{aligned}\mathbf{L}_B &= \left[\frac{d}{dt}(\mathbf{F}_B^e\mathbf{F}_B^i)\right](\mathbf{F}_B^e\mathbf{F}_B^i)^{-1} = \left[\dot{\mathbf{F}}_B^e\mathbf{F}_B^i + \mathbf{F}_B^e\dot{\mathbf{F}}_B^i\right](\mathbf{F}_B^i)^{-1}(\mathbf{F}_B^e)^{-1} \\ &= \dot{\mathbf{F}}_B^e(\mathbf{F}_B^e)^{-1} + \mathbf{F}_B^e\dot{\mathbf{F}}_B^i(\mathbf{F}_B^i)^{-1}(\mathbf{F}_B^e)^{-1} = \mathbf{L}_B^e + \mathbf{F}_B^e\mathbf{L}_B^i(\mathbf{F}_B^e)^{-1} = \mathbf{L}_B^e + \tilde{\mathbf{L}}_B^i\end{aligned} \tag{8}$$

where the velocity gradient $\mathbf{L}$ can be decomposed into the sum of stretch rate and spin tensors, $\mathbf{D}$ and $\mathbf{W}$ respectively:

$$\mathbf{L}_B^i = \dot{\mathbf{F}}_B^i(\mathbf{F}_B^i)^{-1} = \mathbf{D}_B^i + \mathbf{W}_B^i \tag{9}$$

$$\tilde{\mathbf{L}}_B^i = \tilde{\mathbf{D}}_B^i + \tilde{\mathbf{W}}_B^i \tag{10}$$

The unloading process, which relates the deformed state with the intermediate relaxed state, is not uniquely defined; since an arbitrary rigid body rotation of the intermediate state still leaves the state stress free (Bergström et al., 2002). To ensure the unloading unique, the viscous spin tensor is prescribed zero, i.e. $\tilde{\mathbf{W}}_B^i = 0$, according to (Bergström and Boyce, 1998; Bergström et al., 2002). The rate of inelastic deformation of Network B is constitutively prescribed by:

$$\tilde{\mathbf{L}}_B^i = \tilde{\mathbf{D}}_B^i = \dot{\gamma}_B\mathbf{N}_B \tag{11}$$

where:

$$\mathbf{N}_B = \frac{\mathrm{dev}[\mathbf{T}_B]}{\tau} = \frac{\mathrm{dev}[\mathbf{T}_B]}{\|\mathrm{dev}[\mathbf{T}_B]\|_{\mathbf{F}}} \tag{12}$$

provides the direction of the driving stress state of the relaxed configuration and $\dot{\gamma}_B$ is an effective creep rate. $\tau = \|dev[\mathbf{T}_B]\|_{\mathbf{F}}$ is the effective stress, which drives the viscous flow. The time derivative of $\mathbf{F}_B^p$ can be derived as follows:

$$\tilde{\mathbf{L}}_B^i = \mathbf{F}_B^e\dot{\mathbf{F}}_B^i(\mathbf{F}_B^i)^{-1}(\mathbf{F}_B^e)^{-1} = \dot{\gamma}_B\mathbf{N}_B \tag{13}$$

and:

$$\dot{\mathbf{F}}_B^i = \dot{\gamma}_B(\mathbf{F}_B^e)^{-1}\frac{\mathrm{dev}[\mathbf{T}_B]}{\|\mathrm{dev}[\mathbf{T}_B]\|_{\mathbf{F}}}\mathbf{F}_B^e\mathbf{F}_B^i \tag{14}$$

The effective creep rate-equation for viscous flow is given by Bergström and Boyce (1998) and Bergström et al. (2002):

$$\dot{\gamma}_B = \dot{\gamma}_0 \left(\overline{\lambda_B^i} - 1 + \xi\right)^C \left[R\left(\frac{\tau}{\tau_{base}} - \hat{\tau}_{cut}\right)\right]^m \tag{15}$$

where $\dot{\gamma}_0 = 1$ (s^{-1}) is a constant introduced to ensure dimensional consistency. $R(x) = [(x + |x|)/2]$ is the ramp function. τ_{base} represents the flow resistance. m is a positive stress exponential and C is a strain exponential constant, which is restricted at the interval $[-1, 0]$ (Bergström and Boyce, 1998). ξ is a strain adjustment factor, which was introduced in a later work (Bergström et al., 2002) to eliminate the singularity of Eq. (15) (note that $\overline{\lambda_B^i} \geqslant 1$) and maintaining all features of the original equation. $\hat{\tau}_{cut}$ is a cut-off stress such that only elastic strains will occur for values lower than the cut-off stress. This last parameter was shown by Bergström (2012) and Banić et al. (2012) and Eq. (15) corresponds to adaptation of the original Bergström–Boyce model. The chain stretch in the inelastic part of Network B is given by:

$$\overline{\lambda_B^i} = \sqrt{\frac{\mathrm{tr}\left[\mathbf{F}_B^i \mathbf{F}_B^{i^T}\right]}{3}} \tag{16}$$

4. Materials and methods

Suture fibers of PLA–PCL (composition 90:10; initial number average molecular weight M_{n_0} of 28,000; polydispersion of 3.3; glass transition temperature Tg of 56 °C and melting temperature Tm of 157 °C, with 400 μm in diameter) were provided by *Chirmax*.

First, non degraded specimens were evaluated. Test specimens of 100 mm long were cut for each experimental set. The distance between the machine test grips was set to 50 mm and, non degraded specimens were monotonically quasi-static tensile tested. The experiments were carried out under displacement rates of 500 mm/min and 15 mm/min in a universal testing machine (TIRAtest 2705) with a load cell of 500 N and grips commonly used in fiber testing. In addition to these monotonic tensile tests, quasi-static cyclic test was done by using the same setup under a load displacement rate of 50 mm/min and unload displacement rate of 5 mm/min. The first cycle was loaded up to 0.7 mm, then reloaded up to 1.5 mm, 3 mm, 4.5 mm and 6 mm in the 5th cycle. The unloading between each cycle was conducted until reach a stress free state. It is important to highlight that this first set of tests was used to verify the potentialities of Bergström–Boyce model to simulate the time-dependent mechanical behavior for the investigated biodegradable polymer.

Second, the fiber specimens were placed in 50 ml test tubes and submitted to four different degradation steps (0 weeks, 2 weeks, 4 weeks and 8 weeks) under phosphate buffer solution (PBS) at constant temperature (37 °C). Similar quasi-static monotonic tensile tests under displacement rate of 250 mm/min were performed on dry specimens (24 h in incubator at 37 °C) at the end of each degradation step. It is important to observe that this second set of tests was used to calibrate the model at each degradation step.

The experimental results until rupture, published in previous work (Vieira et al., 2013, 2011a), exposed the nonlinear time-dependent mechanical behavior of PLA–PCL suture fibers. Based on these results (the average of three tests), inverse analyses to identify the parameters of the model was carried out by using MCalibration™ software (from *Veryst Engineering*). The calibration technique used to minimize the difference between the experimental results and the model predictions was the Nelder–Mead method, which is implemented in the MCalibration™ software. In addition, a parametric study for all the parameters was performed by using three sets of values (low, mean and high), where the mean corresponds to the value determined by calibration, and the low and high values correspond to deviations around 10 percent of the mean value. This parametric study enabled to identify the most sensitive parameters of the material model for the prediction of the experimental results. After that, another calibration was done, based on the same set of monotonic tests, where the two active parameters were those most sensitive, while the other ones were set to averaged values obtained by the previous calibration. After determining the two most sensitive parameters at each degradation step, they were fitted by linear regression as function of the degradation damage $d(t, u)$ model defined by Vieira et al. (2011a). Finally, the model results by using the two most sensitive parameters at each degradation step, calculated by the correspondent linear regression, were compared to the experimental results. It is important to highlight that only the results of monotonic tensile tests at 250 mm/min were used in the analyses to identify the parameters of the model during hydrolytic degradation.

5. Results and discussion

In the Fig. 4, it is possible to observe that the evaluated model was able to simulate the time-dependent response of the polymer in this range of strain rates (500 mm/min and 15 mm/min). By using these two loading cases in the calibration, the coefficient of determination R^2 was very close to 1 (one), meaning that the model was able to predict very accurately the mechanical behavior of the polymer at different strain rates.

In the Fig. 5, it is verified that the evaluated model was also able to simulate the hysteric effect, commonly observed in polymers. By

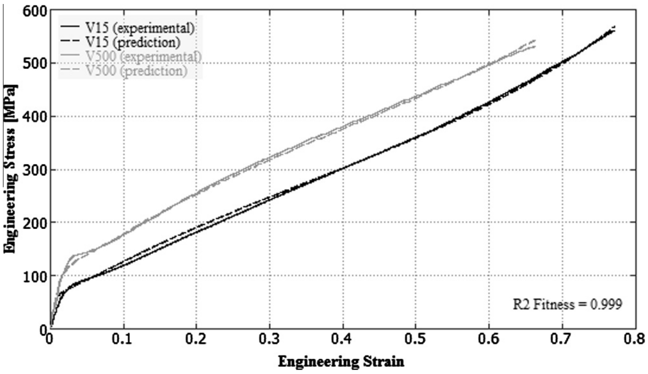

Fig. 4. Experimental results of monotonic tensile test at two displacement rates (500 and 15 mm/min) of non degraded PLA–PCL fiber, and model results via Bergström–Boyce model.

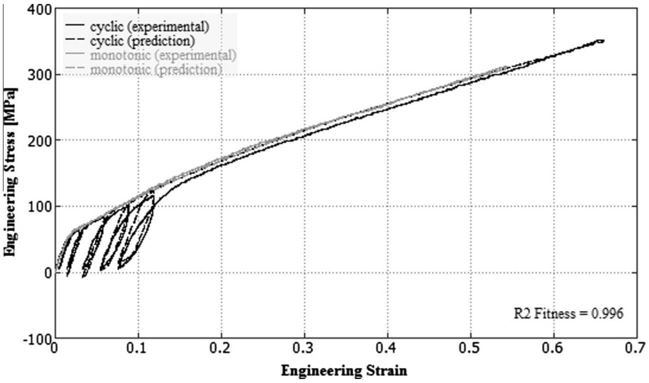

Fig. 5. Experimental results of cyclic tensile test of non degraded PLA–PCL fiber, and model results via Bergström–Boyce model.

using cyclic unloading–reloading and monotonic loading cases in the calibration, the coefficient of determination R^2 was still very close to 1 (one).

From Figs. 6–9, it is shown that the evaluated model could simulate the non-linear mechanical behavior until rupture in monotonic tensile test at different hydrolytic degradation steps, because the coefficient of determination R^2 is always above 0.995. Although, its precision is slightly reduced with hydrolytic degradation time. Comparing to hyperelastic models such as the Neo-Hookean or the Arruda–Boyce models, the coefficient of determination R^2 does not reach 0.98, and reduces considerably in function of the hydrolytic degradation time (R^2 does not reach 0.8 weeks after 8 weeks of hydrolytic degradation). Thus, the coefficient of determination is much higher for the Bergström–Boyce model. For example, after 8 weeks of hydrolytic degradation, R^2 is 0.995.

In the Table 1, a list of the material model parameters, which were identified by calibration, are presented at each degradation step.

Based on the parametric study, it is concluded that the shear modulus μ is the most sensitive parameter of the Bergström–Boyce model, for all hydrolytic degradation steps. In the Fig. 10, it is possible to observe different model results, when the shear modulus μ value is deviated more or less 10 percent of the value determined by calibration. As other thermoplastics, this material is nearly incompressible and hence it is very sensible to distortions.

In the Fig. 11, it is possible to verify that the locking stretch λ_L is another sensitive parameter for the non degraded specimens, because small deviations in this parameter may affect the model results, mainly at higher strain levels. This is due to the fact that the value determined by calibration (1.56) is close to the actual stretch (around 1.6). This leads to an asymptotic increase in stress for stretch values ($\lambda = 1 + \varepsilon$) close to or higher than the locking stretch λ_L. In the Fig. 11, it is possible to verify that this parameter affects the hardening prediction at higher strain levels when the stretch is higher than the locking stretch λ_L. Hence, replacing this value by $\lambda_L = 5$ (instead of 1.56), and considering a higher shear modulus μ (408 instead of 355, as shown in Table 2), the predicted result is nearly the same. This increase of the locking stretch (that induces a decrease of the hardening prediction) is compensated by a higher shear modulus (that induces an increase of the hardening prediction). Since the locking stretch value, determined by the calibration for the hydrolytic degraded specimens, was higher than 5, this parameter becomes almost insensitive. For example, after two weeks of hydrolytic degradation, predictions of the mechanical behavior of the polymer are not affected, as it can be seen in the Fig. 12.

According to the parametric study, also the flow resistance τ_{base} is sensitive to deviations, as shown by Fig. 13. Although it is much less sensitive than the shear modulus μ, it is observed great changes of its value during the degradation process. This is due to the increased in brittleness and internal dynamic friction between molecules, with consequent increase of resistance to flow. On the other hand, stress exponential m is also sensitive to deviations, but its value remains in the same order of magnitude.

The strain exponential C is nearly insensitive for values close to zero. The correlation with experimental results decreases for values close to -1 (minus one). This same trend was observed by Bergström et al. (2002) in the case o UHMWPE, where the

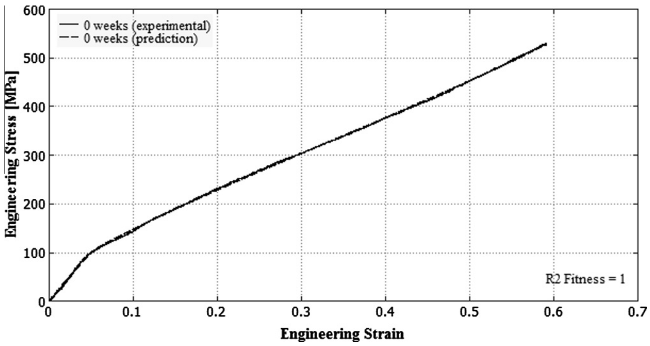

Fig. 6. Experimental results of monotonic tensile test at 250 mm/min of non degraded PLA–PCL fiber, and model results via Bergström–Boyce model.

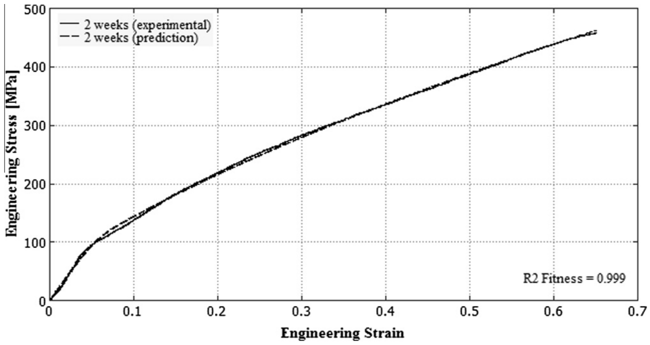

Fig. 7. Experimental results of monotonic tensile test at 250 mm/min of PLA–PCL fiber, and model results via Bergström–Boyce model, after two weeks of hydrolytic degradation.

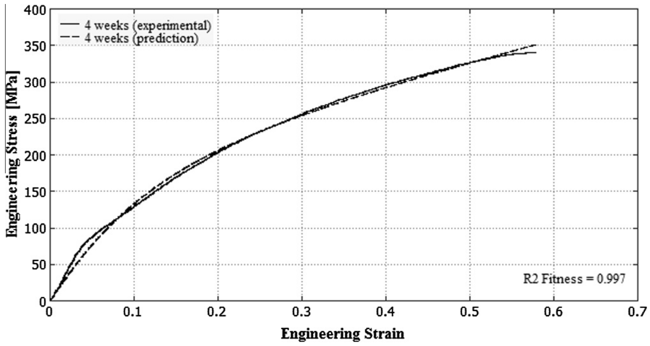

Fig. 8. Experimental results of monotonic tensile test at 250 mm/min of PLA–PCL fiber, and model results via Bergström–Boyce model, after four weeks of hydrolytic degradation.

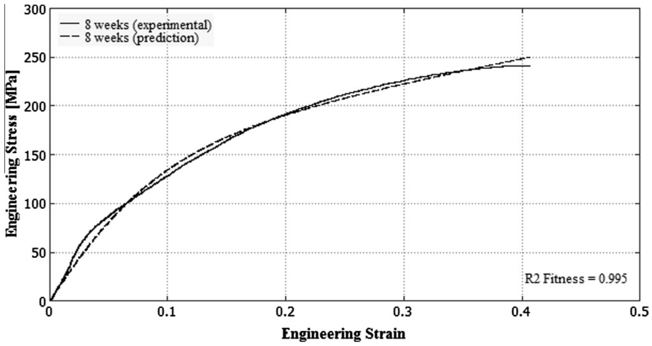

Fig. 9. Experimental results of monotonic tensile test at 250 mm/min of PLA–PCL fiber, and model results via Bergström–Boyce model, after eight weeks of hydrolytic degradation.

Table 1
List of the material model parameters identified by calibration at each hydrolytic degradation step.

Model parameters	0 weeks	2 weeks	4 weeks	8 weeks
μ – Shear modulus of network A (MPa)	355.439	331.842	256.811	192.686
λ_L – Locking stretch	1.55813	5.18064	9.99997	5.42087
κ – Bulk modulus (MPa)	59137.1	52603.8	2522.86	10961.5
s – Relative stiffness of network B	0.994461	1.03951	1.40451	2.27284
ξ – Strain adjustment factor	0.286773	0.189326	0.500236	0.482787
C – Strain exponential	−0.48398	−0.54034	−0.00815	−1.8e−08
τ_{base} – Flow resistance (MPa)	48.2916	94.9219	1645.91	1402.44
m – Stress exponential	13.4184	5.68314	1.1001	1.34039
$\hat{\tau}_{cut}$ – Normalized cut-off stress for flow	0.008102	0.009484	4.17e−06	0.003313

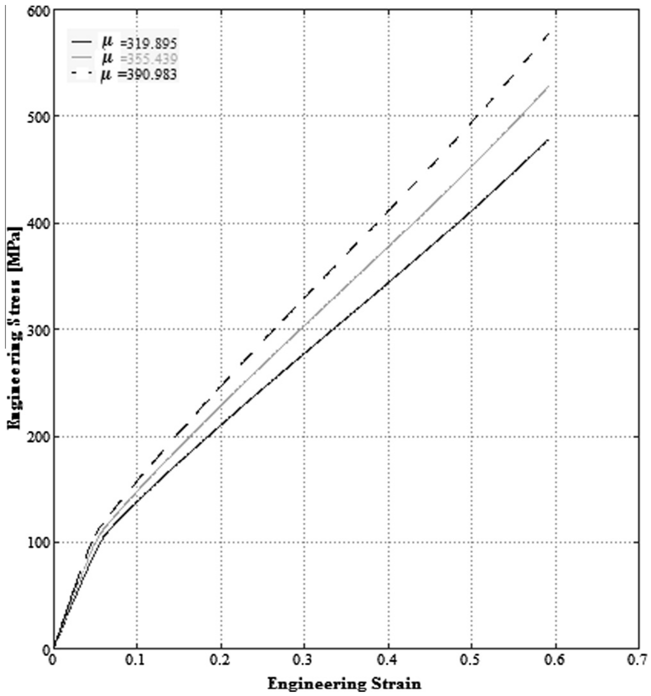

Fig. 10. Model results of the Bergström–Boyce model, with deviation around 10% of the shear modulus μ identified by calibration, for the non degraded specimen.

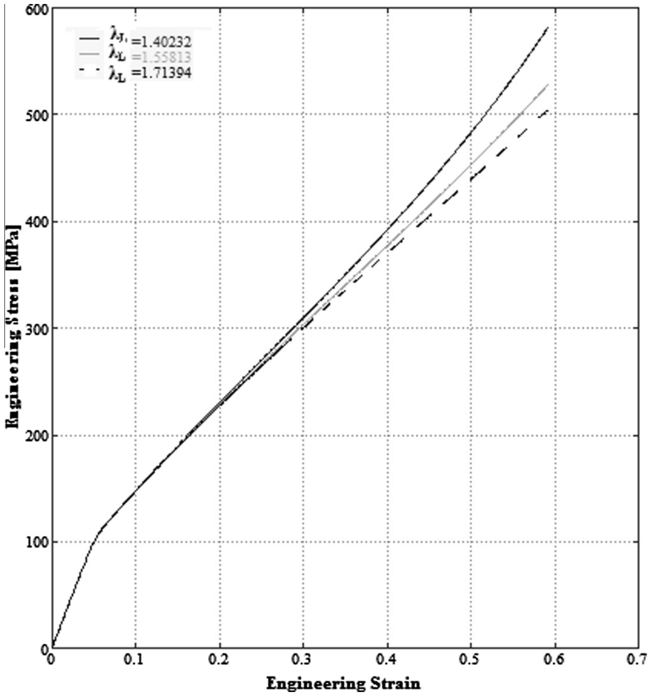

Fig. 11. Model results of the Bergström–Boyce model, with deviation around 10% of the locking stretch λ_L identified by calibration, for the non degraded specimen.

optimal value of the material parameter C was very close to zero. For thermoplastics, it is possible to consider $C = 0$. This will simplify the effective creep rate-equation (Eq. (15)) without significantly affecting the accuracy of predictions. However, for elastomeric materials, the same parameter C has a value close to -1 (minus one) (Bergström and Boyce, 1998). Hence the magnitude of the plastic flow rate is nearly independent on the strain level.

Considering these observations, another calibration of parameters was performed, based on the same set of monotonic test, but only these two parameters were investigated: the shear modulus μ and the flow resistance τ_{base}. The other parameters were set constant during the hydrolytic degradation process, assuming averaged values identified from the different hydrolytic degradation steps, which were calculated in the previous calibration. The parameters identified by this method are shown in Table 2. As it can be observed, the material was assumed to be nearly incompressible, since the bulk modulus κ used, which represents the resistance to volume changes, is very high from the beginning of the hydrolytic degradation process until eight weeks. Furthermore, higher values of shear modulus produce a negligible effect on the model results, and lower values decrease the correlation between the model and the experimental results. It was observed that the shear modulus decreases nearly linear as function of the hydrolytic damage. This same trend was also reported in a previous work (Vieira et al., 2011a), where the neo-Hookean, Mooney–Rivlin and second reduced hyperelastic models were used to predict the mechanical behavior of the same biodegradable polymer. Muliana and Rajagopal (2012) also assumed in their own viscoelastic model that shear modulus decreases with hydrolytic degradation, i.e. hydrolytic degradation process softens the polymers. On the order hand, Soares (2008) reported that the material becomes less viscous during hydrolytic degradation, and returns faster to a relaxed state. This assumption is also consistent to the results of this work, where the flow resistance τ_{base} increases nearly linear with the hydrolytic damage. This could be explained due to the increased brittleness of the material in function of the degradation process, as observed in the graphics for monotonic loadings. Therefore, based on these experimental results, as well as on the calibration method, is

Table 2
List of the material model parameters identified by calibration at each hydrolytic degradation step, with only two active parameters (the shear modulus μ and the flow resistance τ_{base}).

Model parameters	0 weeks	2 weeks	4 weeks	8 weeks
μ – Shear modulus of network A (MPa)	408.062	335.217	261.177	211.162
λ_L – Locking stretch	5	5	5	5
κ – Bulk modulus (MPa)	30,000	30,000	30,000	30,000
s – Relative stiffness of network B	1.5	1.5	1.5	1.5
ξ – Strain adjustment factor	0.4	0.4	0.4	0.4
C – Strain exponential	−0.25	−0.25	−0.25	−0.25
τ_{base} – Flow resistance (MPa)	32.109	139.271	209.505	287.162
m – Stress exponential	3	3	3	3
$\hat{\tau}_{cut}$ – Normalized cut-off stress for flow	0.005	0.005	0.005	0.005

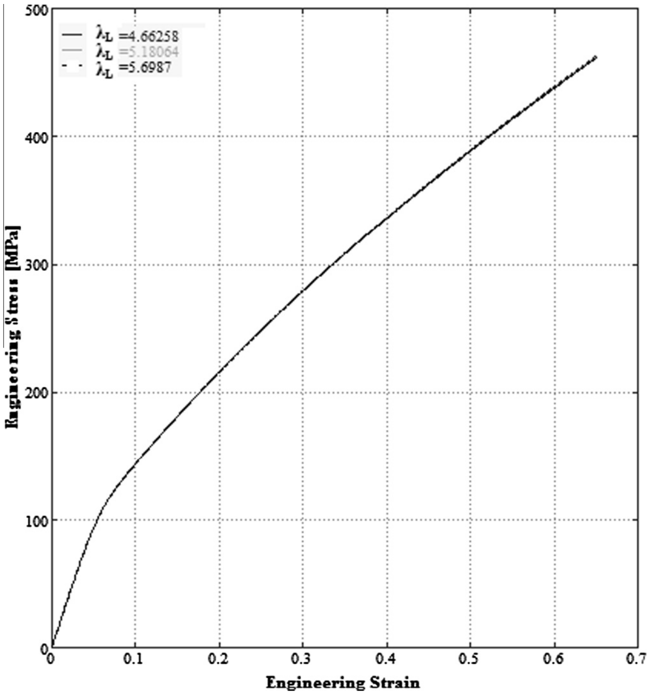

Fig. 12. Model results of the Bergström–Boyce model, with deviation around 10% of the locking stretch λ_L identified by calibration, for the specimen after two weeks of hydrolytic degradation.

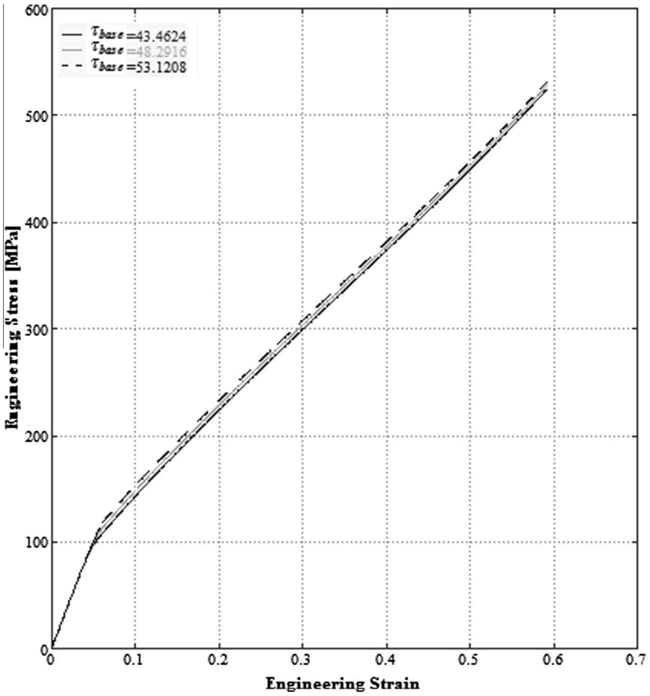

Fig. 13. Model results of the Bergström–Boyce model, with deviation around 10% of the flow resistance τ_{base} identified by calibration, for the non degraded specimen.

possible to assume that the material will become less viscous. As mentioned earlier, some researchers have observed experimentally this phenomenon.

The linear fitting of these two parameters (the shear modulus μ and the flow resistance τ_{base}) as function of the hydrolytic damage d is shown in the Fig. 14. A good correlation of the linear fitting was demonstrated, because the coefficient of determination R^2 is above 0.97 for both parameters. Based on these linear equations, the shear modulus $\mu(d)$ and the flow resistance $\tau_{base}(d)$ were calculated, and they are shown in Table 3. Then these values were used together with other material model parameters values previously assumed constant during hydrolytic degradation, in order to predict the mechanical behavior of the polymer. The basic assumption in this formulation consists on the introduction of the hydrolytic damage scalar field, which does not change the formulation of the constitutive law, and the model still exhibits the same constitutive behavior at any hydrolytic degradation step. A comparison of these model results against the experimental monotonic tensile test results, at different hydrolytic degradation steps, is shown in Figs. 15–18. Although the result of these predictions, by using the proposed method to estimate the material model parameters, is less accurate than the initial model results, by using the calibration of all the parameters, the result has still a satisfactory correlation, because the coefficient of determination R^2 is above 0.98. This good correlation is due to the fact that calibration and validation of model results are based on the same monotonic test results. This correlation would decrease, if the model results were validated by using other types of experimental tests, such as cyclic loadings. However, based on this method, two of the parameters are functions of the hydrolytic damage d, while the other parameters remain constant during hydrolytic degradation.

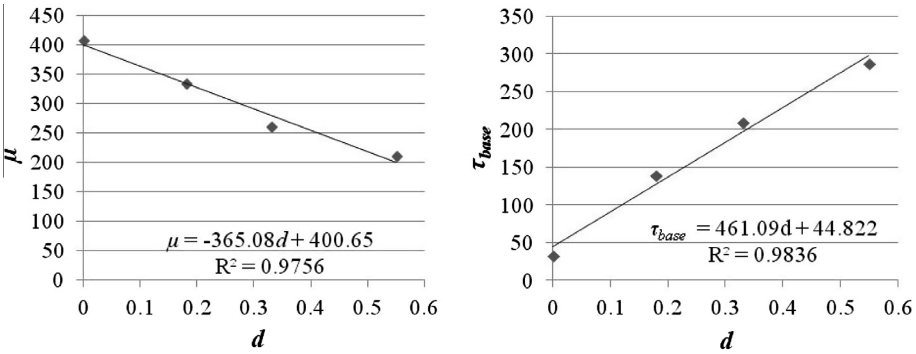

Fig. 14. Evolution of the material parameters of the Bergström–Boyce model, shear modulus μ and flow resistance τ_{base}, during hydrolytic degradation.

Table 3
List of the shear modulus μ and the flow resistance τ_{base} used at each hydrolytic degradation step, determined by the linear fitting equation as function of hydrolytic damage.

Model parameters	0 weeks	2 weeks	4 weeks	8 weeks
μ – Shear modulus of network A (MPa)	400.65	334.936	280.174	199.856
τ_{base} – Flow resistance (MPa)	44.822	127.818	196.982	298.422

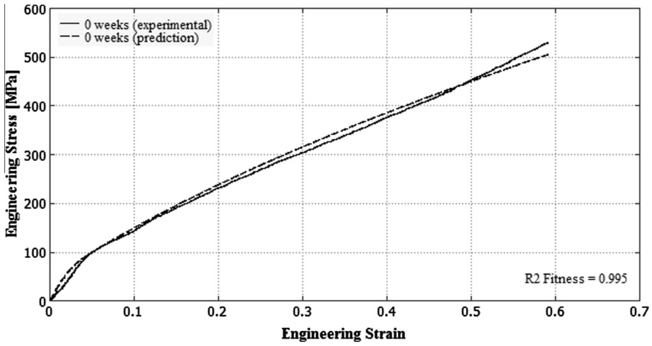

Fig. 15. Experimental results of monotonic tensile test at 250 mm/min of non degraded PLA–PCL fiber, and model results via Bergström–Boyce model.

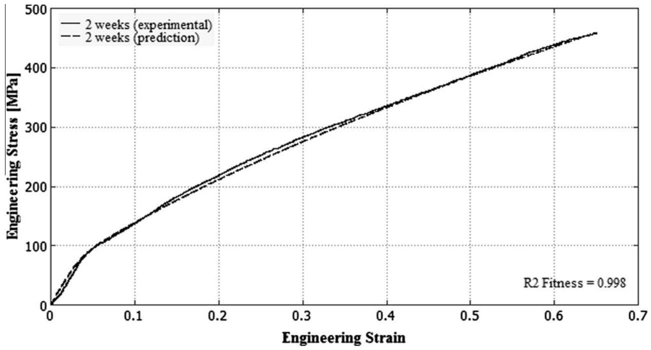

Fig. 16. Experimental results of monotonic tensile test at 250 mm/min of PLA–PCL fiber, and model results via Bergström–Boyce model, after two weeks of hydrolytic degradation.

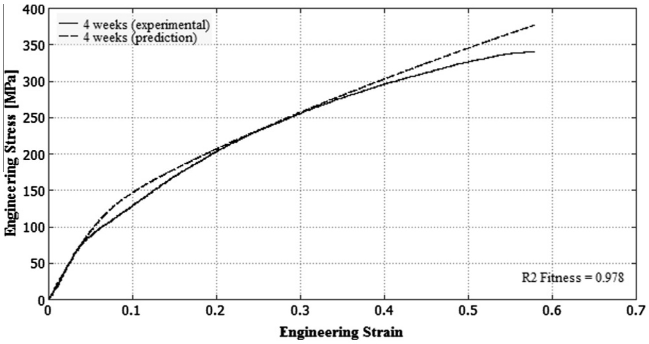

Fig. 17. Experimental results of monotonic tensile test at 250 mm/min of PLA–PCL fiber, and model results via Bergström–Boyce model, after four weeks of hydrolytic degradation.

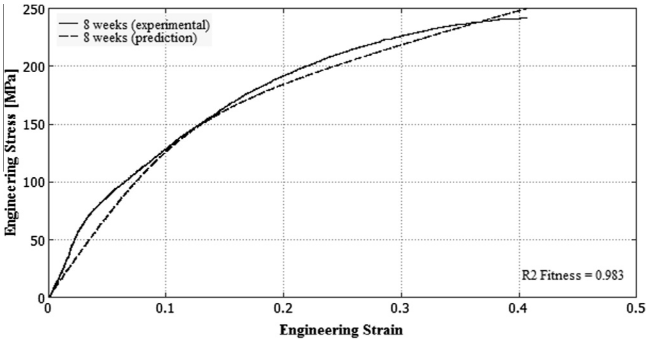

Fig. 18. Experimental results of monotonic tensile test at 250 mm/min of PLA–PCL fiber, and model results via Bergström–Boyce model, after eight weeks of hydrolytic degradation.

6. Conclusions

Biodegradable polymers, as conventional polymers are known by their non-linear and time-dependent mechanical behavior, as shown by the experimental results. The method presented in this work is the first one based on a time-dependent constitutive model validated experimentally for large deformations. Although the application of this method was given for this particular blend, the authors had verified the applicability of the present method for other biodegradable polymers, such as PDO and PGA. Furthermore, it can be extended to other thermoplastic biodegradable materials.

Considering the parametric studies, it is possible to conclude that the three-dimensional constitutive model analyzed in this study was able to predict the time-dependent behavior of PLA–PCL blend under hydrolytic degradation. The shear modulus μ and the flow resistance τ_{base} become linear functions of the hydrolytic damage, while the other material model parameters remain constant during the hydrolytic degradation process. The variations in some parameters of the model are related to the calibration and the convergence to an optimal set of values. As proved, variations of these parameters do not affect the prediction and may be compensated by the variation of other sensitive parameters. At the end this is a phenomenological model, albeit the method is physically inspired on the hydrolysis random scission kinetics. Comparing to experimental results at different hydrolytic degradation steps, the model results were accurate until more than half life ($d = 0.5$). Above this value, the assumption of homogeneous degradation process and constant hydrolytic degradation rate do not hold. Although the Bergström–Boyce model was originally developed for engineering rubbers, it was successfully used to predict the mechanical behavior of other thermoplastics and other soft materials with both non-linear and time-dependent mechanical behavior. Albeit this model is much more complex than the hyperelastic models, which is usually applied to model the mechanical behavior of biodegradable polymer, it enables to simulate realistic loading cases similar to those in service. These in service loading cases comprise loading at various rates, and cyclic loading above yielding. On that ground, the investigated material model is able to simulate more relevant phenomena that occur in biodegradable polymers, such as relaxation and creep, hysteresis and inelastic strain with hydrolytic biodegradation. This was confirmed by using the proposed method to predict the mechanical behavior of biodegradable polymers based on the Bergström–Boyce constitutive model.

On the whole, the proposed method can provide new insights to the design and dimensioning of biodegradable devices, such as scaffolds, according to mechanical and durability requirements. The simple modeling technique presented here allows preclinical evaluation of the functional compatibility, and the optimization by comparison of different solutions in terms of long-term biomechanical behavior. These constitutive models can be implemented in commercial finite element software and the material parameters can be changed as function of hydrolytic damage. In addition, a failure criterion could be associated with these parameters. These can be also applied to more complicated numerical models in 3D applications.

Finally, the method proposed is only valid for low thickness devices, or porous structures, in the first stages of erosion, and without considering the hydrolytic degradation rate dependence on temperature, environment and stress state. Further model improvements should consider these dependencies, as well as the crystalline degree dependence, the diffusion of water, enzymes and biodegradation products. In these more complex problems, hydrolytic damage will depend not only on the biodegradation time, but also on the water concentration and the hydrolysis kinetic parameter; no longer constants but depending on time, geometry, biodegradation media, temperature and stress state. In these cases, hydrolytic damage will be a local internal variable, which varies along the volume and must be calculated previously at each material point and at each biodegradation step. However, the proposed adaptation of the studied constitutive model is still valid from there forward.

Acknowledgments

André C. Vieira wishes to thank CAPES/CNPq (Young Talents Program – Grant number: 022/2012). The authors would like to highlight that this work was also partially supported by the Program USP/UP, which is a scientific cooperation agreement established between the University of Porto (Portugal) and the University of São Paulo (Brazil). The author Rui M. Guedes also acknowledge the support under the grant PTDC/EME-PME/114808/2009 provided FCT (Portuguese Science and Technology Foundation). Finally, the authors wish to thank the reviewer's comments and suggestions which really helped to improve the quality of the manuscript.

References

Arruda, E.M., Boyce, M.C., 1993a. A three-dimensional constitutive model for the large stretch behavior of rubber elastic materials. J. Mech. Phys. Solids 41, 389–412.

Arruda, E.M., Boyce, M.C., 1993b. Evolution of plastic anisotropy in amorphous polymers during finite straining. Int. J. Plast. 9, 697–720.

Banić, M.S., Stamenković, D.S., Miltenović, V.D., Milošević, M.S., Miltenović, A.V., Djekić, P.S., Rackov, M.J., 2012. Prediction of heat generation in rubber or rubber–metal springs. Therm. Sci. 16, S527–S539.

Bardenhagen, S.G., Stout, M.G., Gray, G.T., 1997. Three-dimensional, finite deformation, viscoplastic constitutive models for polymeric materials. Mech. Mater. 25, 235–253.

Bellenger, V., Ganem, M., Mortaigne, B., Verdu, J., 1995. Lifetime prediction in the hydrolytic ageing of polyesters. Polym. Degrad. Stab. 49, 91–97.

Bergstrom, J.S., 2012. PolyUMod – A Library of Advanced User Materials. Veryst Engineering, LLC, Need-ham, Mass, USA.

Bergström, J., Boyce, M.J., 1998. Constitutive modeling of the large strain time-dependent behavior of elastomers. Mech. Phys. Solids 46, 931–954.

Bergström, J.S., Kurtz, S.M., Rimnac, C.M., Edidin, A.A., 2002. Constitutive modeling of ultra-high molecular weight polyethylene under large-deformation and cyclic conditions. Biomaterials 23, 2329–2343.

Boyce, M.C., Parks, D.M., Argon, A.S., 1988. Large inelastic deformation of glassy polymers. I. Rate dependent constitutive model. Mech. Mater. 7, 15–33.

Chu, C.C., 1985. Strain-accelerated hydrolytic degradation of synthetic absorbable sutures. In: Hall, C.W. (Ed.), Surgical Research, Recent Developments: Proceedings of the First Annual Scientific Session of the Academy of Surgical Research, firsst ed. Pergamon Press, San Antonio, pp. 111–115.

Dafalias, Y.F., 1991. Constitutive model for large viscoelastic deformations of elastomeric materials. Mech. Res. Commun. 18, 61–66.

Drozdov, A.D., Gupta, R.K., 2003. Constitutive equations in finite viscoplasticity of semicrystalline polymers. Int. J. Solids Struct. 40, 6217–6243.

Fancello, E., Ponthot, J.P., Stainier, L., 2006. A variational formulation of constitutive models and updates in non-linear finite viscoelasticity. Int. J. Numer. Methods Eng. 65, 1831–1864.

Farrar, D.F., Gilson, R.K., 2002. Hydrolytic degradation of polyglyconate B: the relationship between degradation time, strength and molecular weight. Biomaterials 23, 3905–3912.

Ferry, J.D., 1980. Viscoelastic Properties of Polymers. John Wiley and Sons, New York.

Flory, P.J., 1977. Theory of elasticity of polymer networks. The effect of local constraints on junctions. J. Chem. Phys. 66, 5720–5729.

Gan, Z., Yu, D., Zhong, Z., Liang, Q., Jing, X., 1999. Enzymatic degradation of poly(ε-caprolactone)/poly(DL-lactide) blends in phosphate buffer solution. Polymer 40, 2859–2862.

Garlotta, D.A., 2001. Literature review of poly(lactic acid). J Polym. Environ. 9, 63–84.

Göpferich, A., 1996. Mechanisms of polymer degradation and erosion. Biomaterials 17, 103–114.

Göpferich, A., Langer, R., 1993. Modeling of polymer erosion. Macromolecules 26, 4105–4112.

Grabow, N., Bunger, C.M., Sternberg, K., 2007. Mechanical properties of a biodegradable balloon-expandable stent from poly (L-lactide) for peripheral vascular application. ASME J. Med. Devices 1, 84–88.

Harren, S.V., 1995. Toward a new phenomenological flow rule for orientationally hardening glassy polymers. J. Mech. Phys. Solids 43, 1151–1173.

Hasan, O.A., Boyce, M.C., 1995. A constitutive model for the nonlinear viscoplastic behavior of glassy polymers. Polym. Eng. Sci. 35, 331–344.

Hausler, K., Sayir, M.B., 1995. Nonlinear viscoelastic response of carbon black reinforced rubber derived from moderately large deformations in torsion. J. Mech. Phys. Solids 43, 295–318.

Holzapfel, G., 1996. A new viscoelastic constitutive model for continuous media at finite thermomechanical changes. Int. J. Solids Struct. 33, 3019–3034.

Huntley, H.E., Wineman, A.S., Rajagopal, K.R., 1996. Chemorheological relaxation, residual stress and permanent set arising in radial deformation of an elastomeric hollow sphere. Math. Mech. Solids 1, 267–299.

James, H.M., Guth, E., 1943. Theory of the elastic properties of rubber. J. Chem. Phys. 11, 455–481.

Johnson, A.R., Quigley, C.J., Freese, C.E., 1995. A viscohyperelastic finite element model for rubber. Comput. Methods Appl. Mech. Eng. 127, 163–180.

Khan, K.A., El-Sayed, T., 2012. A phenomenological constitutive model for the nonlinear viscoelastic responses of biodegradable polymers. Acta Mech. 224, 287–305.

Li, S., Garreau, H., Vert, M., 1990. Structure-property relationships in the case of the degradation of massive aliphatic poly (α-hydroxyacids) in aqueous media. Part 2: degradation of lactide/glycolide copolymers: PLA37.5GA25 and PLA75GA25. J. Mater. Sci. Mater. Med. 1, 131–139.

Lubarda, V.A., Benson, D.J., Meyers, M.A., 2003. Strain-rate effects in rheological models of inelastic response. Int. J. Plast. 19, 1097–1118.

Lunt, J., 1998. Large-scale production, properties and applications of polylactic acid polymers. Polym. Degrad. Stab. 59, 145–152.

Miehe, C., Göktepe, S., Lulei, F., 2004. A micro-macro approach to rubber-like materials—Part I: The non-affine micro-sphere model of rubber elasticity. J. Mech. Phys. Solids 52, 2617–2660.

Miller, N.D., William, D.F., 1984. The in vivo and in vitro degradation of poly(glycolic acid) suture material as a function of applied strain. Biomaterials 5, 365–368.

Moore, J.E., Soares, J.S., Rajagopal, K.R., 2010. Biodegradable stents: biomechanical modeling challenges and opportunities. Cardiovascul. Eng. Technol. 1, 52–65.

Muliana, A., Rajagopal, K., 2012. Modeling the response of nonlinear viscoelastic biodegradable polymeric stents. Int. J. Solids Struct. 49, 989–1000.

O'Dowd, N.P., Knauss, W.G., 1995. Time dependent large deformation of polymers. J. Mech. Phys. Solids 43, 771–792.

Rajagopal, K.R., Wineman, A.S., 1992. A constitutive equation for nonlinear solids which undergo deformation induced microstructural changes. Int. J. Plast. 8, 385–395.

Rajagopal, K.R., Srinivasa, A.R., Wineman, A.S., 2007. On the shear and bending of a degrading polymer beam. Int. J. Plast. 23, 1618–1636.

Reese, S., Govindjee, S., 1998. A theory of finite viscoelasticity and numerical aspects. Int. J. Solids Struct. 35, 3455–3482.

Rubin, M.B., 1987. An elastic–viscoplastic model exhibiting continuity of solid and fluid states. Int. J. Eng. Sci. 9, 1175–1191.

Shaw, J.A., Jones, A.S., Wineman, A.S., 2005. Chermorheological response of elastomers at elevated temperatures: experiments and simulations. J. Mech. Phys. Solids 53, 2758–2793.

Smeulders, S.B., Govindjee, S., 1999. A phenomenological model of an elastomer with an evolving molecular weight distribution. J. Rheol. 43, 393–414.

Soares, J.S., 2008. Constitutive Modeling for Biodegradable Polymers for Applications in Endovascular Stents (PhD Dissertation). Mechanical Engineering Texas A&M University.

Soares, J., Rajagopal, K.R., Moore, J.E., 2010. Deformation induced hydrolysis of a degradable polymeric cylindrical annulus. Biomech. Model Mech. 9, 177–186.

Treloar, L.R., 1975. The Physics of Rubber Elasticity. Oxford University Press Inc., New York.

Tsuji, H., Ikada, Y., 1998. Properties and morphology of poly(L-lactide)—II Hydrolysis in alkaline solution. J. Polym. Sci. A Polym. Chem. 36, 59–66.

Tsuji, H., Ikada, Y., 2000. Properties and morphology of poly(L-lactide) 4. Effects of structural parameters on long-term hydrolysis of poly(L-lactide) in phosphate-buffered solution. Polym. Degrad. Stab. 67, 179–189.

Tsuji, H., Nakahara, K., 2001. Poly(L-lactide)—IX Hydrolysis in acid media. J. Appl. Polym. Sci. 86, 186–194.

Vieira, A.C., Guedes, R.M., Marques, A.T., 2009. Development of ligament tissue biodegradable devices: a review. J. Biomech. 42, 2421–2430.

Vieira, A.C., Vieira, J.C., Guedes, R.M., Marques, A.T., 2010. Degradation and viscoelastic properties of PLA–PCL, PGA–PCL, PDO and PGA fibres. Mater. Sci. Forum, 636–637, 825-83242.

Vieira, A.C., Vieira, J.C., Ferra, J., Magalhães, F.D., Guedes, R.M., Marques, A.T., 2011a. Mechanical study of PLA–PCL fibres during in vitro degradation. J. Mech. Behav. Biomed. 4, 451–460.

Vieira, A.C., Marques, A.T., Guedes, R.M., Tita, V., 2011b. Material model proposal for biodegradable materials. Proc. Eng. 10, 1597–1602.

Vieira, A.C., Medeiros, R., Guedes, R.M., Marques, A.T., Tita, V., 2013. Visco-elastic–plastic properties of suture fibers made of PLA–PCL. Mater. Sci. Forum 730–732, 56–61.

Wall, F.T., Flory, P.J., 1951. Statistical thermodynamics of rubber elasticity. J. Chem. Phys. 19, 1435–1439.

Williams, D.F., 1981. Enzymatic hydrolysis of polylactic acid. Proc. Inst. Mech. Eng. H 10, 5–7.

Wineman, A., Min, J.H., 2002. Time-dependent scission and cross-linking in an elastomeric cylinder undergoing circular shear and heat conduction. Int. J. Nonlinear Mech. 38, 969–983.

Zdunek, A.B., 1993. Theory and computation of the steady state harmonic response of viscoelastic rubber parts. Comput. Methods Appl. Mech. Eng. 105, 63–92.